Transactions of the KSNVE, 23(12) : 1035~1044, 2013
http://dx.doi.org/10.5050/KSNVE.2013.23.12.1035

한국소음진동공학회논문집 제23권 제12호, pp. 1035~1044, 2013
ISSN 1598-2785(Print), ISSN 2287-5476(Online)

Fluid-structure Interaction Analysis of Large Sandwich Panel Structure for Randomly Distributed Wind Load considering Gust Effects

거스트 영향이 고려된 랜덤 분포 풍하중에 대한 대형 샌드위치 패널 구조물의 유체-구조 연성해석

Dae Woong Park†
박 대 웅

(Received July 23, 2013 ; Revised October 30, 2013 ; Accepted November 28, 2013)

Key Words : Fluid-structure Interaction(유체-구조 연성해석), Random Distributed Wind Load(랜덤분포 풍하중), RANS turbulence model(RANS 난류모델)

ABSTRACT

Because of the high specific stiffness and strength inherent in the sandwich structure composed of facesheet that resists in-plane loads and a core that resists out-of-plane loads, it is often used for large and light-weighted structures. However, inevitably the increased flexibility allows greater deformation-based disturbances in the structures. Thus, it is necessary to analyze the structural safety. To obtain more accurate analytical results, the input disturbances must more closely simulate real load conditions; to improve accuracy, non-linear elements such as gust effects were considered. In addition, the structural safety was analyzed for the iso-grid sandwich panel structure using fluid–structure interactions. For a more realistic simulation, flow velocity fields, which consider the effects of irregular gust fluctuation, were generated and the coupled field was analyzed by mapping the pressure and displacement.

요 약

면내 하중을 지지하는 면재와 면외 하중을 지지하는 심재로 구성되는 샌드위치 패널 구조물은 높은 비강도와 비강성을 가지므로 경량화가 요구되는 대형 구조물에 자주 이용된다. 그러나, 이러한 구조물은 필연적으로 높은 하중에 대하여 유연성의 증가를 일으키게 되므로, 이에 대한 구조 안전성 분석이 이루어져야 한다. 이에 대해 실제 풍하중은 거스트 영향 등을 비롯한 비선형성을 가지는 요소들이 고려되어야 하며, 구조물의 안전성 분석을 위하여 입력 하중에 대해 보다 실제 물리현상에 근접하게 모사되어야 한다. 이에 이 연구에서는 유체-구조 연성해석 기법을 이용하여 대형 등격자-보강 패널 구조물에 대한 구조 안전성 분석이 수행되었다. 입력하중인 풍하중에 대하여 보다 실제적 모사를 위해 불규칙 변동 속도성분인 거스트 영향이 고려된 랜덤분포 풍하중에 대한 유동장을 생성하여 압력-변위 사상을 통하여 연성해석이 수행되었다.

† Corresponding Author ; Member, Mechanical Engineering Team, Reliability Headquarter, Korea Testing & Research Institute
E-mail : dwpark@ktr.or.kr
Tel : +82-32-570-9762, Fax : +82-32-575-5620

‡ Recommended by Editor Hyung-Jo Jung

Nomenclature

K_{zr} : Altitude distribution coefficient for wind velocity
K_{zt} : Additional wind speed coefficient
k : Turbulence kinetic energy
ε : Turbulence dissipation rate

1. Introduction

With the recent global weather change, the frequency of the occurrence of large typhoons has increased, and owing to the increase in the maximum wind speeds of typhoons, support structures with improved ability to withstand greater wind loads are required. Wind, which is one of the disturbances for a structure, is represented by random data, and displays complex and irregular behavior depending on time and altitude; there is no periodicity in wind behavior over a particular time interval. Because of its variability, the effects of wind on structures are applied using statistical methods, and that shows the uniqueness mathematically. Wind speed is divided into average wind speed, which shows equal distribution per unit time, and variable wind speed, which shows irregular distribution. Gusts are a representative example of variable wind speed. In analyzing real structures, randomly distributed wind loads must be included; irregular, but realistic, winds cause numerous difficulties.

Meanwhile, sandwich panel structures, which are widely used in large light structures, are composed of face bars that support the in-plane load, and heartwood, which supports the out-of-plane load. However, when these structures experience high exterior loads, which is characteristic of structures, increased flexibility occurs, and further analysis of structural safety must be performed. In addition, for accurate structural safety analysis, the input loading should be more closely considered relative to the actual physical phenomenon.

Many studies have been performed related to large-scale structural wind analysis. Large-scale structural analysis was performed for wind loading by Jeong et al[1]. In the study, the wind load was considered; however, for the structural analysis, the mapping procedure between the pressure and deformation was not carried out, and gust effects were not considered in the application of wind loads. The effects of turbulence viscosity with respect to wind loads were considered by Han et al[2,3]; however, the procedure for mapping wind pressure to structural deformation was not considered.

Therefore, in this study, variable effects were considered, relative to the use of a large liquid storage structure composed of sandwich panels, and to randomly distributed input wind loads that accounted for the irregular velocity changes inherent in gust effects. Based on this, a flow field was produced and pressure-displacement mapping technique was applied to illustrate the stress distribution in the structural analysis field. Additionally, structural safety analysis of an actual large liquid storage unit, made of grid-reinforced panels, was performed. The k–ε model proposed by Scott-Pomerantz[7] was used to model the turbulence viscosity effects of the interface between the structural surface and the fluid.

2. Developing of Design Wind Load with Gust

2.1 Random Distributed Wind Load

Generally, when wind load is interpreted as an exterior input load, it is done by considering only the average wind speed, and assuming that the load condition is static. However, the actual physical phenomenon that takes place more closely relates to a random distribution of wind loads, and to obtain the most accurate model possible, random distributed wind loading that includes varia-

ble wind speed, must be considered. These conditions are required because variable wind speeds are dynamic loads that induce vibration effects on the structure. Variable wind speed is the irregular velocity component that rapidly changes per unit time, and can be modeled as a spectrum function with variable frequency distribution characteristics. From the point of view of structural safety, the total wind load can be represented by static wind loads modeled using average wind speed and dynamic wind loads modeled using variable wind speeds. Static wind loads are divided into drag, dynamic lift, and torsional moment components, and the static wind power coefficient is determined using the average wind speed and sectional form. Through static interpretation and analysis, the structure's response behavior is determined. Alternatively, static wind loads can also be divided into self-excited vibration loads resulting from the interaction of wind pressure and the resistant structural forces and dynamic loads represented by turbulence components. The resulting response of the structure can then be determined through dynamic interpretation. To determine the response for irregular, variable wind speed effects, frequency field interpretation is generally used; however theoretically, the frequency field interpretation method can only be applied when the load–displacement relationship is linear. The time history of variable wind speed in a time field interpretation should be used to account for the correlation of two points in a space via cross-spectrum analysis.

When producing an actual, large-scale structure, if it is based on specific regulations or design standards, similar equivalent interpretation methods with smaller inherent operational costs are appropriated. Similar equivalent interpretation is a method of resolving more complex wind loads into uniform loads and their structural responses based on static and dynamic wind loading. Interpretation using the similar equivalent method works by determining the design wind speed through regional characteristics similar in nature to the target application. Speeds are calculated at environmental conditions and their effects are evaluated relative to engineering characteristics. Ulti- mately, the equivalent wind pressure is calculated from the kinetic energy equation of designed wind speed. In other words, the variable wind speed affects the gust coefficient, and the gust coefficient regulated in the design standard is assigned to the wind pressure to calculate the wind load. The gust coefficient is calculated through the interaction of variable wind speeds and the structure, and therefore, the general gust coefficient provided in design standards cannot be the appropriate number. Additionally, the complex analysis involving application of gust effects is generally avoided for less critical designs; however, to ensure a design is safe in most diverse conditions, application of complex gust effects is necessary. In this study, wind pressure interpretation was performed based on the results of fluid analysis of the actual maximum design wind speeds.

2.2 Wind Load Design Criteria

This study concerns the effects of wind loads on large-scale structures, as defined by the wind load design standards, "structure load standard" and "structure standard," from KBC 2005[12] and ASCE 7-05[13]. The dominant factors related to wind loads are the geographical location, shape of the structure, and surface conditions; to consider these factors, various values of surface roughness, high distribution coefficients, and additional wind speed coefficients must be calculated.

Various values of surface roughness are a parameter showing the change in wind speed per geographic illumination and are classified into four stages. A Class is assigned to areas in the center of big cities with tall buildings exceeding 10 floors, B Class is for areas concentrated with houses 3.5 m tall as well as middle-story build-

ings, C Class ratings are reserved for areas concentrated with 1.5~10 m tall obstacles and low-story buildings, and D Class terrain has almost no obstacles. D Class consists of obstacles less than 1.5 m tall; seaside or coastal plains, grasslands, and airports are suitable examples of D Class ratings. To calculate the wind pressure based on the measured height, designed wind speed distributions as follows.

$$V_z = V_0 K_{zr} K_{zt} I_w \tag{1}$$

$$K_{zr} = 0.96 Z^{\alpha} \tag{2}$$

In Equations (1) and (2), V_0 is the designed wind speed for a random height, and it is the basic wind speed of all areas; K_{zr} is the largest distribution coefficient of wind speed; K_{zt} is the additional wind speed coefficient; and I_w is the importance coefficient of the structure. The largest distribution coefficient of the wind speed, the coefficient changing based on surface condition of the installed location of the structure and height is same as in Table 1, and calculated as Eq. (2). Here, Z_G is the gradient wind level height, and α is the vertical distribution coefficient.

After determining the various values of terrain roughness of the area in which the structure resides, the design coefficients are determined, and in the most unfavorable state, roughness is assigned a Class D rating. The gradient wind height of the structure in this study was 250 m, the vertical distribution coefficient, α, was 0.10, Z_b was 5 m, Z was 10 m, and Z_G was 250 m. The resulting maximum distribution coefficient was 1.0286.

The coefficient that considered tilt angle effects was the additional wind speed coefficient. For the structure's surrounding environment, an additional wind speed coefficient, Z_{zt}, was determined using Table 3, and the importance coefficient, I_w, was determined by considering the structure's function. Using this process, the structure's designed wind speed was determined.

Table 1 Coefficient for height above ground level

Height above ground level Z(m)	Exposure			
	A	B	C	D
$Z \leqq Z_b$	0.58	0.81	1.0	1.13
$Z_b < Z \leqq Z_G$	0.22 Z^{α}	0.45 Z^{α}	0.71 Z^{α}	0.96 Z^{α}

Table 2 Coefficient of vertical distribution

Height above ground level Z(m)	Exposure			
	A	B	C	D
Z_b	20 m	15 m	10 m	5 m
Z_G	500 m	400 m	300 m	250 m
α	0.33	0.22	0.15	0.10

Table 3 Extra wind coefficient for slope

Severe slope for wind load(φ)	Extra coefficient for wind(Z_{zt})	
	Incline ($\varphi_d \leqq 0.05$)	Hill or mountain ($\varphi_d \geqq 0.05$)
0.05	1.05	1.11
0.1	1.09	1.21
0.2	1.18	1.41
$\geqq$ 0.3	1.27	1.61

2.3 Randomly Distributed Design Wind Loads Considering Gust Effects

Generally, wind characteristics show random distributions, which are inherent in dynamic wind effects consisting of average, and variance terms. The gust coefficient is expressed as the rate of dynamic effects for static effects for each member of the structure. The large, lightweight structure composed of sandwich-type panels used in the current study, which is flexible structure sensitive to wind loads, has large gust coefficient values. In addition, the wind characteristics differ based on the shape of a structure, and therefore, gust coefficients vary according to the sectional form. Because this structure is flexible and sensitive to wind characteristics, the gust coefficient based on various terrain roughness values cannot be applied as it is; it must be modified.

The wind pressure shows the amount of kinetic

energy acting on the surface per unit area, and the designed speed pressure, q_z, of the wind speed change is expressed in Eq. (3). Here, p is the air density, which depends on temperature, pressure, and humidity. However, strong winds from typhoons mainly occur in summer and do not have a profound effect at other times. Therefore, assuming a constant value of 0.125 kgf-s^2/m^4 is reasonable, and then the designed speed pressure, q_z, can be calculated using Eq. (3).

On the other hand, wind pressure is applied per unit area of the structure. The designed wind pressure, p, can be expressed using the wind power, C_f, gust coefficient, G_f, and the designed speed pressure, q_z, as shown in Eq. (4). The gust coefficient, G_f, which represents the dynamic response of the structure, can generally be presented in terms of the various values of surface roughness. Using this process, the designed wind pressure, p, was calculated. The designed wind pressure of large structures must satisfy the regulation stating that such structures must be able to withstand wind pressure loads of at least 50 kgf/m^2. This regulation can be found in Term 1 of "Regulations of structural standard of a building."[13] The design wind load is expressed as a wind pressure area multiplied by design wind pressure, as shown in Eq. (5). Wind pressure area is the effective cross-sectional area in which the wind load is applied, and thus, the load is applied to the wind pressure area vertically.

$$q_z = \frac{1}{2}\rho v_z^{\,2} \tag{3}$$

$$p = C_f G_f q_z \tag{4}$$

$$p = \rho A \tag{5}$$

To actually apply the randomly distributed wind load, physical quantity shown structural dynamic behavior occurred by the turbulence of the wind is required. This can be defined using a statistically determined coefficient, which describes the maximum displacement in a set of averaged values. In addition, the gust coefficient depends not only on a structure's sectional form, but also on the unique frequency changes relative to stiffness and mass of the structure. This coefficient is also influenced by the unique frequency mode, and therefore, for final structure designs, wind analysis must be performed using numerical methods, such as physical experiments or computational fluid dynamics(CFD). From this result, the effects of gust-imposed loads are found.

Table 4 The gust effect factor for the roughness

Roughness for exposure	A	B	C	D
Gust effect factor(G_f)	2.5	2.2	1.9	1.8

For the structure and surrounding air, the flow field analysis results using CFD are as follows. To consider gust effects, and to express the Reynolds stress using viscosity, a concept provided by Boussinesq, the turbulence model was imposed into the flow field analysis process. As shown in Eqs. (6) and (7), a k–ε model was used for the turbulence model. Additionally, k and ε were converted in the base of the turbulence strength of the flow field. Although its applications are limited, the k–ε model is the main model used to describe turbulence effects. In addition, the model is economic with respect to arithmetic costs, superior in numeric safety, and predicts generally excellent results, and therefore, it was as a used method in the engineered turbulence flow field.

$$\frac{\partial}{\partial t}(pk) + \frac{\partial}{\partial x_i}(\rho u_i k) = \frac{\partial}{\partial x_i}\left(\frac{u_i}{\sigma_i}\frac{\partial k}{\partial x_i}\right) + G + G - \rho\varepsilon \tag{6}$$

$$\frac{\partial}{\partial t}(p\varepsilon) + \frac{\partial}{\partial x_i}(\rho u_i \varepsilon) = \frac{\partial}{\partial x_i}\left(\frac{m_i}{\sigma_c}\frac{\partial \varepsilon}{\partial x_i}\right) + C_{1c}\frac{\varepsilon}{k} + (G_k + 1 - C_{3c})G_b) - C_{2c}\rho\frac{\varepsilon^2}{k} \tag{7}$$

Where, $G_k = \mu_s(\frac{\partial u_j}{\partial x_i} + \frac{\partial u_i}{\partial x_j})\frac{\partial u_j}{\partial x_i}$

$$G_b = -g_i(\frac{\mu_s}{\rho\sigma_s} + \frac{\partial \rho}{\partial x_i})$$

3. FSI Analysis for the Large Sandwich Panel Structure

3.1 Flow Field Analysis of Large Sandwich Panel Structure

Based on the calculated design wind load from the above process, flow field analysis was performed for the large sandwich panel structure. The iso-grid sandwich panel structure shown in Fig. 1 is the subject of the analysis.

For the design wind loading conditions, flow analysis of the same load on the front and side faces was performed. The results of the analysis for the pressure and velocity distributions in the front-loaded wind case for a large liquid storage tank are shown in Figs. 2 and 3. In addition, the velocity and pressure distributions for the maximal side-loaded wind condition are shown in Figs. 4 and 5. The maximum pressure of the wind load in the normal direction equal to 3921 Pa was occurred on the side of the holding tank. The maximum wind speed for the same scenario was

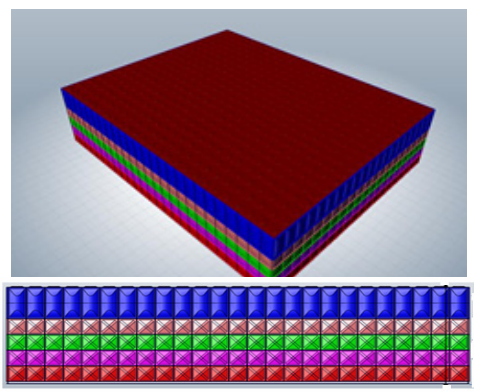

Fig. 1 Iso-grid sandwich panel structure

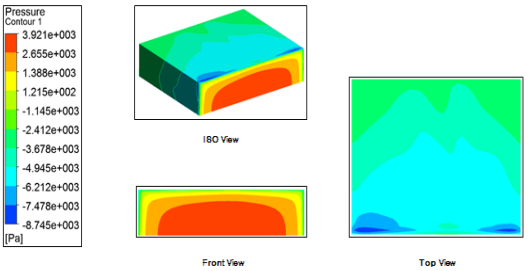

Fig. 2 Pressure distribution in large sandwich panel structure for maximum front wind load

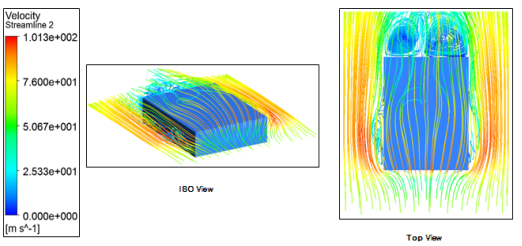

Fig. 3 Flow velocity field in large sandwich panel structure for maximum front wind load

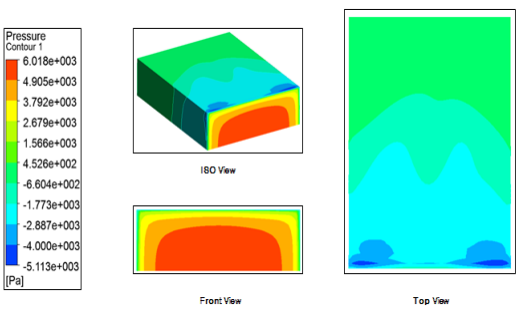

Fig. 4 Pressure distribution in large sandwich panel structure for maximum side wind load

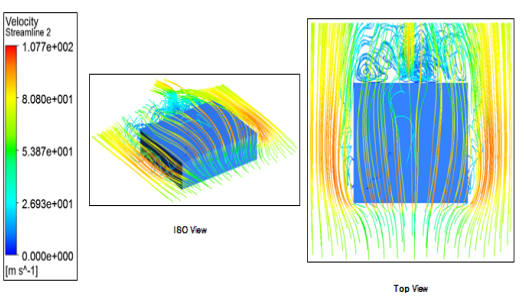

Fig. 5 Flow velocity field in large sandwich panel structure for maximum side wind load

101.3 m/s. On the other hand, the maximum pressure in the side-loaded design case occurred on the side of the liquid tank, similar to the normal direction. The maximum pressure was 6018 Pa, and the maximum wind speed was 107.7 m/s.

3.2 Fluid - structure Interaction Analysis of the Large Liquid Storage Tank

Using the flow field analysis results, the finite element model given in Fig. 6 was created for structural safety analysis of the large liquid storage tank. Fluid–structure ductility analysis was then performed. For the finite element model, shell elements were used for the relatively thin frames. For the grid stiffener, equivalent shell-type elements were used. For the delicate stay-bolt component, which incurred concentrate stress levels, solid elements were used.

Using mapping pressure distribution and displacement in the normal direction of the large liquid storage tank, ductile analysis was performed to calculate the displacement and stress distributions. The results for these simulations are shown in Figs. 7 and 8. The maximum stress occurred in the stay-bolt of the storage tank structure; its von Mises stress level was approximately 50 MPa.

Thus, because the yield stress of the stay-bolt material is 215 MPa, the maximum stress did not cause any plastic deformation. Furthermore, because the stay-bolt was not loaded beyond its elastic limit, the design is sufficiently safe, from a structural integrity point of view.

As a result of the fluid–structure ductility analysis in the side-loaded direction, it was determined that the part incurring maximum stress was a component in the frame connecting the liquid storage tank to the supports, as shown in Figs. 9 and 10. The von Mises stresses in the connection component of the frame were 128 MPa; thus, given that the yield stress of the material is 230 MPa, the structure is safe in side-loaded design cases. The highest stress level in any direction was greater than the stress in the normal direction; however, even in the side-loaded scenario (direction of maximum stress), the structural stiffness was sufficient and the resulting design was determined to be safe.

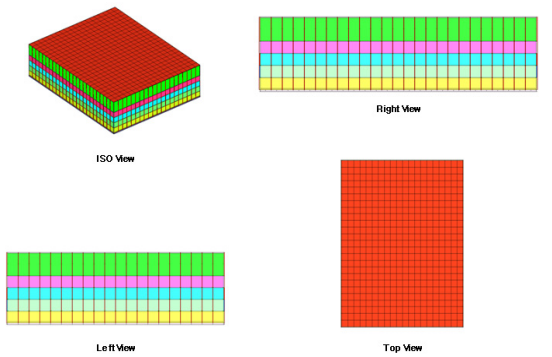

Fig. 6 Finite element model for large sandwich panel structure

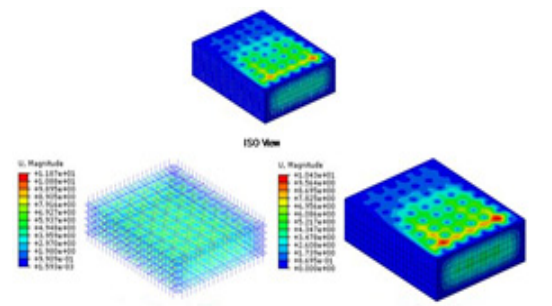

Fig. 7 Displacement distribution in large sandwich panel structure for front wind load

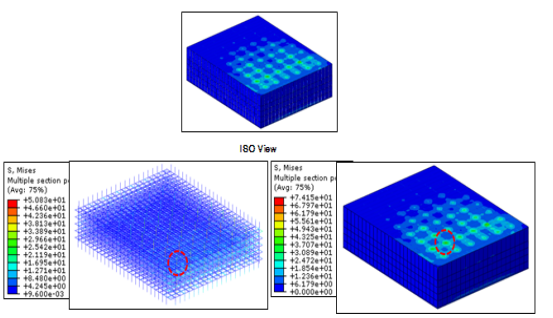

Fig. 8 Von Mises stress distribution in large sandwich panel structure for front wind load

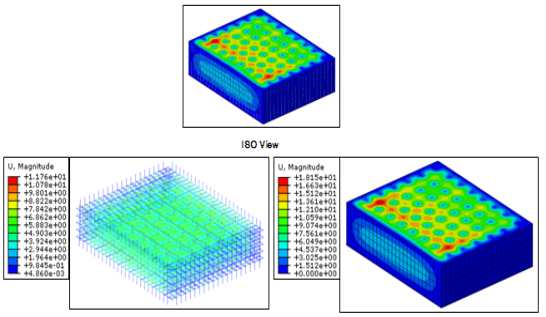

Fig. 9 Displacement distribution in large sandwich panel structure for side wind load

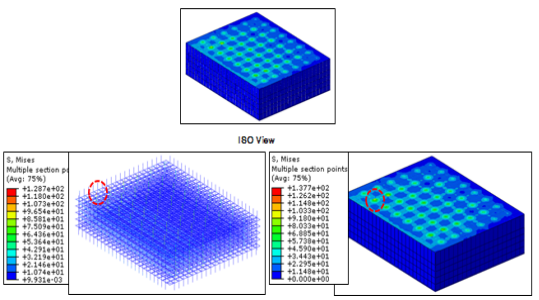

Fig. 10 Von Mises stress distribution in large sandwich panel structure for side wind load

Table 5 Analysis result for the front wind load

FSI analysis result	
Max pressure[Pa]	3921
Max wind speed[m/sec]	101.3
Max von Mises stress[MPa]	50
Max stress region	Stay bolt part
Max displacement[mm]	10.4
Safety factor	3.3

Table 6 Analysis result for the side wind load

FSI analysis result	
Max pressure[Pa]	6018
Max wind speed[m/sec]	107.7
Max von Mises stress[MPa]	128
Max stress region	Frame part
Max displacement[mm]	11.8
Safety factor	0.8

As discussed, the FSI analysis results are presented in Table 5 and Table 6. This structure is relatively vulnerable to winds acting from the side; however, it has a positive safety factor found from the stress analysis results. In addition, the regions incurring maximum stresses are reinforced structural members. Thus, the structure is sufficiently designed, with respect to large, lightweight structural standards.

4. Conclusion

In this study, structural safety analysis for large, flexible structures having grid-reinforced panels was performed using fluid–structure ductility analysis. The procedure for calculating the design's wind loads was based on KBC 2005[(12)] and ASCE 7-05[(13)]. For the dominant factors of wind load, geographical location, and structural shape, various surface conditions were considered. Relative to the various conditions of terrain roughness, high distribution coefficients and additional wind speed coefficients were calculated. To more accurately describe the physical phenomena related to actual wind loads imposed on structures, randomly distributed wind loads, which are irregular wind components that are affected by gusts, were considered. Based on the variable wind model, analytical flow fields were been produced and applied with a pressure–displacement mapping method to calculate the stress distribution in the structural analysis area, and structural safety analysis for an actual large, flexible structure using grid-reinforcement panel sandwiched structural members. Using the analysis method proposed in this study, for similar large and flexible structures, improved estimation of the structural safety considering randomly distributed wind loads affected by gusts is possible.

References

(1) Jeong, D. H., Seo, M. S., Kim, D. H., Choi, H.

J., Kim, E. J. and Kang, D. E., 2013, Hydraulic Radome Drive Open-close Equipment CFD Aerodynamic and Structural Analysis, Proceedings of the KSNVE Annual Spring Conference, pp. 352~356.

(2) Han, D.-S. and Han, G.-J., 2011, The Difference in the Uplift Force at Each Support Point of a Container Crane between FSI Analysis and a Wind Tunnel Test, Journal of Mechanical Science and Technology, Vol. 25, No. 2, pp. 301~308.

(3) Han, D. S., Han, G. J. and Kwak, K. S., 2010, Driving Reference Data for Alarm System in a Container Crane by Fluid-structure Analysis, Trans. of the KSME(A), Vol. 34, No. 8, pp. 1091~1096

(4) Kirshman, D. J. and Liu, F., 2006, Flutter Prediction by an Euler Method on Non-moving Cartesian Grids with Gridless Boundary Condition, Computer & Fluids, Vol. 35, No. 6, pp. 571~586.

(5) Chen, X., Zha, G. C. and Hu, Z., 2004, Numerical Simulation of Flow Induced Vibration Based on Fully Coupled Fluid-Structural Interactions, AIAA-2004-2240.

(6) Kim, C. S., Hong, K. S. and Kim, M. K., 2005, Nonlinear Robust Control of a Hydraulic Elevator, Control Engineering Practice, Vol. 13, No. 6, pp. 789~803.

(7) Scott-Pomerantz, C. D., 2004, The K-Epsilon Model in the Theory of Turbulence, PhD. Thesis, University of Pitts-burgh.

(8) Chen, W. Q., Bian, Z. G. and Ding, H. J., 2004, Three-dimensional Vibration Analysis of Fluid-filled Orthotropic FGM Cylindrical Shells, Int. J. of Mechanical Science, Vol. 46, No. 1, pp. 159~171.

(9) Sarhan, K., Zied, D., Hedi, K. and Mohamed, S. A., 2011, Numerical Simulation of Fluid-structure Interaction in a Stirred Vessel Equipped with an Anchor Impeller, Journal of Mechanical Science and Technology, Vol. 25, No. 7, pp. 1749~1760.

(10) Sadeghi, M. and Liu, F., 2005, Coupled Fluid-structure Simulation for Turbomachinery Blade Rows, AIAA 2005-0018.

(11) Ohayon, R. and Soize, C., 2012, Advanced Computational Dissipative Structural Acoustics and Fluid-Structure Interaction in Low-and Medium-Frequency Domains, Reduced Order Models and Uncertainty Quantification, IJASS, Vol. 13, No. 2, pp. 127~153.

(12) Korea Society of Civil Engineering, 2005, Korean Building Code 2005.

(13) American Society of Civil Engineers, 2005, ASCE 7-05.

(14) Kim, D.-H., Oh, S.-W. and Park, O., 2006. Flow-induced Vibration Analysis for Cascades with Stator-rotor Interaction and Viscosity Effect, Transactions of the Korean Society for Noise and Vibration Engineering, Vol. 16, No. 10, pp. 1082~1088

(15) Choi, Y.-S., Lee, J.-H., Jeong, W.-B. and Kim, I.-G., 2010, Dynamic Behavior of Valve System in Linear Compressor based on Fluid-structure Interaction, Journal of Mechanical Science and Technology, Vol. 24, No. 7, pp. 1371~1377.

(16) Kim, Y.-W., 2011, Critical Fluid Velocity of Fluid-conveying Cantilevered Cylindrical Shells with Intermediate Support, Transactions of the Korean Society for Noise and Vibration Engineering, Vol. 21, No. 5, pp. 422~429.

(17) Yoon, K.-J. and Song, O. S., 2010, Flow-induced of Multi-wall Carbon Nano-tubes for Various Boundary Conditions, Transactions of the Korean Society for Noise and Vibration Engineering, Vol. 20, No. 9, pp. 805~815

(18) Kim, Y. W., 2004, Vibration Analysis of Partially Fluid-filled Continuous Cylindrical Shells with Internal Supports, Transactions of the Korean Society for Noise and Vibration Engineering, Vol. 14, No. 3, pp. 244~252.

(19) Jung, K. and Kim, Y.-W., 2012, Free Vibrations of Cylindrical Shells on Partial Plastic Foundations, Transactions of the Korean Society for Noise and Vibration Engineering, Vol. 22, No. 8, pp. 763~770.

(20) White, F. M., 1974, Viscous Fluid Flow, McGraw-Hill, NewYork, pp. 163~189.

(21) Suh, S. H., Choi, Y., Roh, H. W. and Doh, H., 1999, Flow Analysis in the Bifurcated Duct with PIV System and Computer Simulation, Trans. of the KSME(B), Vol. 23, No. 1, pp. 123~180.

(22) Simiu, E. and Scanlan, R. H., 1996, Wind Effects on Structures, 3rd Ed., Wiley-Interscience.

(23) Liu, H., 1991, Wind Engineering - A Handbook

for Structural Engineers, Prentice-Hall.

(24) Teixeira, F. P. and Awruch, M. A., 2005, Numerical Simulation of Fluid-Structure Interaction using the Finite Element Method, Computers & Fluids, Vol. 34, pp. 249~273.

(25) Ministry of Land, Transport and Maritime Affairs of Korean Government, 200, Load Criteria of Building Structures.

(26) Zhou, Y., Karee, A., 2002, On the wind profiles definitions in ASCE 7, J. Struc. Eng.

(27) Ryu, B. J., Jung, S. H. and Kanf, Y. C., 1998, A Study on the Dynamic Stability and Vibration Control of Cantilevered Pipes Conveying Fluid, Transactions of the Korean Society for Noise and Vibration Engineering, Vol. 8, No. 1, pp. 171~179.

(28) Langthjem, M. A. and Olhoff, N., 2003, Modal Expansion of the Perturbation Velocity Potential for a Cantilevered Fluid-conveying Cylindrical Shell, Journal of Fluids and Structures, Vol. 17, No. 1, pp.147~161.

(29) Jeon, S. E., Park, S. H., Byun, Y. H. and Kwon, J. H., 2012, Influence of Compressibility Modification to k-ε Turbulence Models for Supersonic Base Flow, IJASS, Vol. 13, No. 2, pp. 188~198.

(30) Lee, H. and Lee, S., 2011, Convergence Characteristics of Upwind Method for Modified Artificial Compressibility Method, IJASS, Vol. 12, No. 4, pp. 318~330.

(31) Matsuzaki, Y., 2012, An Overview of Flutter Prediction in Tests Based on Stability Criteria in Discrete-Time Domain, IJASS, Vol. 12, No. 4, pp. 305~317.

Dae Woong Park received his B.S. and M.S. degree in Aerospace Engineering from In-ha University, Korea. Mr. Park is currently a senior researcher at Korea Testing & Research Institute. His interests include coupled analysis and optimization, such as FSI, MDO, and topology optimization in the multi-physics field, in addition to reliability-based design optimization.